# Proposal for an Experiment to Measure Mixing, CP Violation and Rare Decays in Charm and Beauty Particle Decays at the Fermilab Collider - BTeV[1]

May 2000

# Executive Summary

[1]Spokespersons: Joel Butler (butler@fnal.gov) and Sheldon Stone (stone@phy.syr.edu)

# 1 Motivation

BTeV is a program designed to challenge the Standard Model explanation of CP Violation, mixing and rare decays in the $b$ and $c$ quark systems. Exploiting the large number of $b$'s and $c$'s produced at the Tevatron collider, we will make precise measurements of Standard Model parameters and an exhaustive search for physics beyond the Standard Model.

BTeV can perform the compelling physics studies that need to be done, and is not limited by current constraints on what studies can be done. We are not constrained by a central geometry that is prescribed to study high $p_t$ physics, nor are we limited by relatively low numbers of $b$-flavored hadrons as in $e^+e^-$ colliders. BTeV excels in several crucial areas including: triggering on decays with purely hadronic final states, charged particle identification, electromagnetic calorimetry and proper time resolution.

In the Standard Model, CP violation has its origin in the phenomenon of quark mixing. As a result, the Standard Model makes very specific connections among various kinds of CP violating $B$ decays and among $B$ decays, kaon and charm decays. Standard Model quark mixing is described by the Cabibbo-Kobayashi-Maskawa matrix [1],

$$\begin{pmatrix} d' \\ s' \\ b' \end{pmatrix} = \begin{pmatrix} V_{ud} & V_{us} & V_{ub} \\ V_{cd} & V_{cs} & V_{cb} \\ V_{td} & V_{ts} & V_{tb} \end{pmatrix} \begin{pmatrix} d \\ s \\ b \end{pmatrix} \quad . \tag{1}$$

The unprimed states are the mass eigenstates, while the primed states denote the weak eigenstates. The $V_{ij}$'s are complex numbers that can be represented by four independent real quantities, if the matrix is unitary. These numbers are fundamental constants of nature that need to be determined from experiment, as with any other fundamental constant such as $\alpha$ or $G$. Measuring them accurately is important, but the most important goal of BTeV is to make a broad range of measurements to check whether the whole picture is correct. If inconsistencies appear, that means there is new physics in play, physics beyond the Standard Model. More detailed study would then elucidate the nature of this new physics.

To confront the Standard Model, measurements are necessary on CP violation in $B^o$ and $B_s$ mesons, $B_s$ mixing, rare $b$ decay rates, and on mixing, CP violation and rare decays in the charm sector. It is possible, perhaps even likely, that the Standard Model mechanism for CP violation and mixing exists but that it is not the whole story. Other mechanisms driven by new physics may be present, perhaps at a low level. The Standard Model has a large number of parameters, mixing angles, masses, and coupling constants, and it is generally believed that the physics should be described in a less *ad hoc* manner via some unknown fundamental principles underlying the model. Once one considers physics beyond the Standard Model one has entered *terra incognita*. Many connections not obvious today may exist. Quark behavior may have analogs or even direct connections to phenomena at much higher energy. Are there relationships between these particles and heavier particles that have not yet been discovered? We note for example that quark mixing as described by the CKM matrix is the first example of mixing of spin-1/2 fermions. Neutrino oscillations suggest that there is an analogous matrix for neutrinos. Are these related? Certainly, these quarks were abundant in the early universe. There is a connection between our studies and Cosmology. As John Ellis recently said "CP violation provides a uniquely subtle link between inner space, as explored by experiments in the laboratory, and outer space, as explored by telescopes measuring the density of matter in the Universe" (CERN courier October 1999).

Although much has been learned about $b$ and $c$ decays from past and current experiments, and more will be learned soon; many, if not most, of the crucial measurements will not have been made by the dawn of the LHC era. It is just as important to see if the "Standard Model" explains quark mixing and CP violation as it is to see if there is a "Standard Model" Higgs particle which generates mass.

With BTeV, we can mount a formidable assault on the CKM explanation of CP violation and mixing. Simply stated, we must do this physics!

# 2 Physics Goals

BTeV is designed to make a complete enough set of measurements on the decays of hadrons containing $b$ and $c$ quarks so as to be able to either accurately determine Standard Model parameters or to discover fundamental inconsistencies that could lead us to an understanding beyond the model. The most important measurements to make involve mixing, CP violation and rare decays of hadrons containing $b$ or $c$ quarks.

Using unitarity, Aleksan, Kayser and London [2] have shown that the CKM matrix can be expressed in terms of four independent phases. These are taken as:

$$\begin{aligned}\beta = arg\left(-\frac{V_{tb}V_{td}^*}{V_{cb}V_{cd}^*}\right), \qquad & \gamma = arg\left(-\frac{V_{ub}^*V_{ud}}{V_{cb}^*V_{cd}}\right), \\ \chi = arg\left(-\frac{V_{cs}^*V_{cb}}{V_{ts}^*V_{tb}}\right), \qquad & \chi' = arg\left(-\frac{V_{ud}^*V_{us}}{V_{cd}^*V_{cs}}\right) \quad .\end{aligned} \tag{2}$$

Another phase $\alpha$, the angle between $V_{ub}$ and $V_{td}$, is redundant with $\beta$ and $\gamma$, since

$$\alpha + \beta + \gamma = \pi \quad . \tag{3}$$

It is important to uniquely measure all of these phases, including $\alpha$. CP asymmetry measurements often involve measuring $\sin(2\phi)$, where $\phi$ is the angle of interest. When we measure $\sin(2\phi)$ we have a four-fold ambiguity in $\phi$, namely $\phi$, $\pi/2-\phi$, $\phi+\pi$ and $3\pi/2-\phi$. These ambiguities can mask the effects of new physics. One of our main tasks is to remove as many of the ambiguities as possible.

A complete program includes measuring the CP violating angles $\alpha$, $\beta$, $\gamma$ and $\chi$, measuring the $B_s$ oscillation frequency, searching for anomalous rates in "rare" $b$ decays and searching for mixing and CP violation in the charm sector, where Standard Model rates are expected to be small and new physics could have large signals.

The "Physics Case," presented in Chapter 1 of the proposal, describes in detail the measurements we wish to make and the specific decay modes that we envision using. Table 1 lists the most important physics quantities and suggested decay modes which measure them.

Table 1: Required CKM measurements for $B$ mesons and associated key detector characteristics.

| Physics Quantity | Decay Mode | Hadron Trigger | $K\pi$ Sep | $\gamma$ Det | Decay Time $\sigma$ |
|---|---|---|---|---|---|
| $\sin(2\alpha)$ | $B^o \to \rho\pi \to \pi^+\pi^-\pi^o$ | $\surd$ | $\surd$ | $\surd$ | |
| $\cos(2\alpha)$ | $B^o \to \rho\pi \to \pi^+\pi^-\pi^o$ | $\surd$ | $\surd$ | $\surd$ | |
| $\mathrm{sign}(\sin(2\alpha))$ | $B^o \to \rho\pi$ & $B^o \to \pi^+\pi^-$ | $\surd$ | $\surd$ | $\surd$ | |
| $\sin(\gamma)$ | $B_s \to D_s^{\pm}K^{\mp}$ | $\surd$ | $\surd$ | | $\surd$ |
| $\sin(\gamma)$ | $B^- \to \overline{D}^0 K^-$ | $\surd$ | $\surd$ | | |
| $\sin(\gamma)$ | $B^o \to \pi^+\pi^-$ & $B_s \to K^+K^-$ | $\surd$ | $\surd$ | | $\surd$ |
| $\sin(2\chi)$ | $B_s \to J/\psi\eta'$, $J/\psi\eta$ | | | $\surd$ | $\surd$ |
| $\sin(2\beta)$ | $B^o \to J/\psi K_S$ | | | | |
| $\cos(2\beta)$ | $B^o \to J/\psi K^o$, $K^o \to \pi\ell\nu$ | | | | |
| $\cos(2\beta)$ | $B^o \to J/\psi K^{*o}$ & $B_s \to J/\psi\phi$ | | | | $\surd$ |
| $x_s$ | $B_s \to D_s^+\pi^-$ | $\surd$ | | | $\surd$ |
| $\Delta\Gamma$ for $B_s$ | $B_s \to J/\psi\eta'$, $D_s^+\pi^-$, $K^+K^-$ | $\surd$ | $\surd$ | $\surd$ | $\surd$ |

We also list the detector characteristics needed to make each measurement. (Rare $b$ decay measurements and charm physics are not included in this table.)

The BTeV detector, described below and in Chapter 2 of the proposal, possesses all of the properties required to carry out these measurements. Perhaps just as importantly, the detector is powerful enough to pursue physics in many areas of $b$ and $c$ production and decay. In the future, new final states that will be important to measure will surely emerge. BTeV, because of its excellent trigger, tracking, particle identification and photon detection, will be in prime position to investigate any such new ideas.

# 3 Rationale for a Forward Detector at the Tevatron

BTeV covers the forward direction, 10-300 mrad, with respect to both colliding beams. In Chapter 2 of the proposal we explain the reasons for this choice. We summarize them here.

Measured $b\bar{b}$ cross-sections at the Tevatron integrate to 100 $\mu$b [3]. One measurement by D0 in the forward region normalizes to 180 $\mu$b [4]. Conservatively, we use the 100 $\mu$b value for our physics projections. The yield of $b$-flavored hadrons then is $\approx 4 \times 10^{11}$ in $10^7$ seconds at a luminosity of $2 \times 10^{32}$ cm$^{-2}$s$^{-1}$ and much of it is in the forward direction. The charm yield is approximately one order of magnitude higher and even more of it is concentrated in the forward direction.

According to QCD calculations of $b$ quark production, there is a strong correlation between the $B$ momentum and pseudorapidity, $\eta$. Shown in Fig. 1 is the $\beta\gamma$ of the $B$ hadron versus $\eta$, as computed by the Monte Carlo physics generator Pythia at $\sqrt{s} = 2$ TeV. It can clearly be seen that near $\eta$ of zero, $\beta\gamma \approx 1$, while at larger values of $|\eta|$, $\beta\gamma$ can easily reach

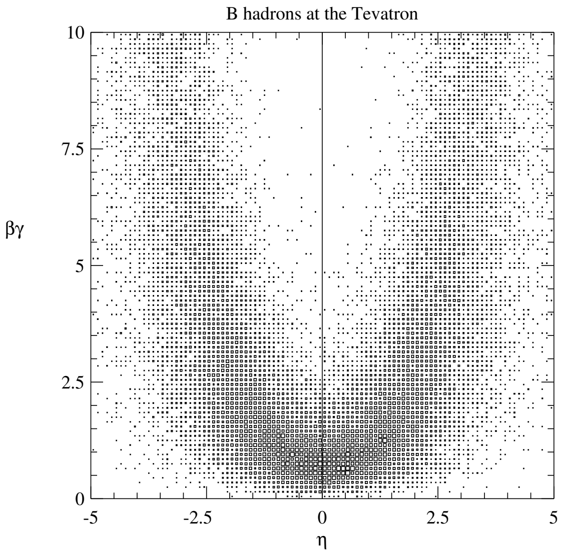


Figure 1: $\beta\gamma$ of the $B$ versus $\eta$.

values of 6. This is important because the mean decay length varies with $\beta\gamma$ and, furthermore, the absolute momenta of the decay products are larger, allowing for a suppression of the multiple scattering error.

A crucially important correlation of $b\bar{b}$ production at hadron colliders is shown in Fig. 2, where the production angle of the hadron containing the $b$ quark is plotted versus the production angle of the hadron containing the $\bar{b}$ quark. Here zero degrees represents the direction of the incident proton and 180 degrees, the incident antiproton. There is a very strong correlation in the proton or the antiproton directions: when the $B$ is forward, the $\overline{B}$ is also forward. (We call both the proton and antiproton directions forward.) This correlation between $B$ and $\overline{B}$ production is not present in the central region (near 90 degrees).

Thus, when a $b$-flavored hadron is produced forward, the accompanying $\bar{b}$ is also produced in the forward direction, allowing for reasonable levels of flavor tagging. The large $b$ quark yield, the long $B$ decay length, the correlated acceptance for both $b$'s and the suppression of multiple scattering errors due to the high $b$ momenta, make the forward direction an ideal choice.

# 4 Detector Description

A sketch of the detector is shown in Fig. 3. The geometry is complementary to that used in current collider experiments. The detector looks similar to a fixed target experiment, but has two arms, one along the proton direction and the other along the antiproton direction.

The key design features of BTeV include:

- A dipole located on the IR, which gives BTeV an effective “two arm” acceptance;

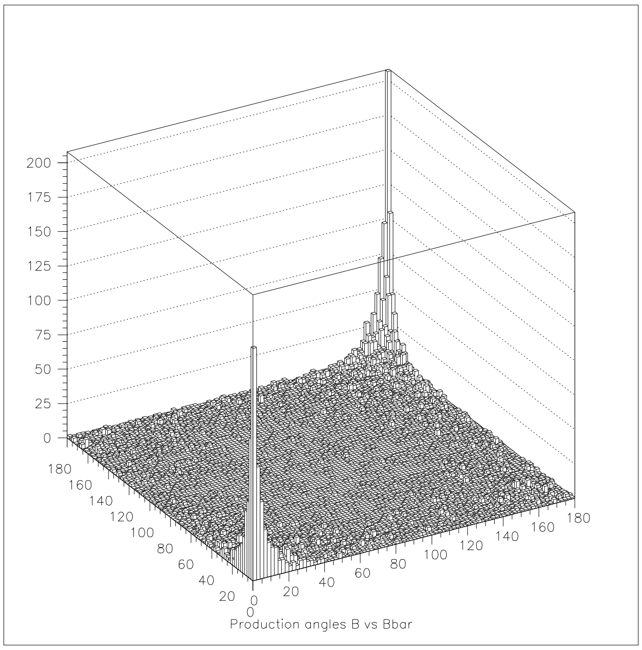


Figure 2: The production angle (in degrees) for the hadron containing a $b$ quark plotted versus the production angle for a hadron containing a $\bar{b}$ quark, from the Pythia Monte Carlo generator.

- A precision vertex detector based on planar pixel arrays;
- A detached vertex trigger at Level 1 that makes BTeV efficient for most final states, including purely hadronic modes;
- Excellent particle identification using a Ring Imaging Cherenkov Detector (RICH);
- A high quality $PbWO_4$ electromagnetic calorimeter capable of reconstructing final states with single photons, $\pi^o$'s, $\eta$'s or $\eta'$'s, and of identifying electrons;
- Precision tracking using straw tubes and silicon microstrip detectors, which provide excellent momentum and mass resolution;
- Excellent identification of muons using a dedicated detector with the ability to supply a dimuon trigger; and
- A very high speed and high throughput data acquisition system which eliminates the need to tune the experiment to specific final states.

Each of these key elements of the detector is discussed in Part 2 of the proposal. Here we discuss them briefly.

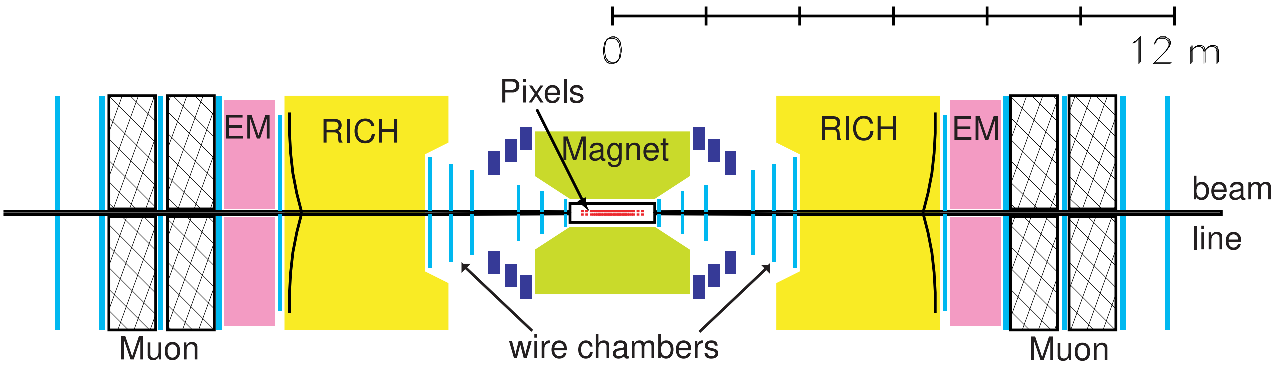


Figure 3: A sketch of the BTeV detector. The two arms are identical.

### 4.1 Dipole Centered on the Interaction Region

A large dipole magnet, with a 1.6 T central field, is centered on the interaction region. In addition to giving us a compact way of providing momentum measurements in both "forward" directions, it provides magnetic deflection in the vertex detector, which is exploited by the trigger to remove low momentum tracks, which could have been deflected by multiple Coulomb scattering, from its search for detached tracks.

### 4.2 The Pixel Vertex Detector

In the center of the magnet there is a silicon pixel vertex detector. This detector serves two functions: it is an integral part of the charged particle tracking system, providing accurate vertex information for the offline analysis; and it delivers very clean, precision space points to the BTeV vertex trigger.

We have tested prototype pixel devices in a beam at Fermilab. These consist of 50 $\mu$m $\times$ 400 $\mu$m pixels bump-bonded to custom made electronics chips developed at Fermilab. A comparison of the position resolution achieved in the test beam and the Monte Carlo simulation is shown in Fig. 4. The resolution is excellent and exceeds our requirement of 9 $\mu$m.

The critical quantity for a $b$ experiment is $L/\sigma_L$, where $L$ is the distance between the primary (interaction) vertex and the secondary (decay) vertex, and $\sigma_L$ is its error. For central detectors the $B$'s are slower, because the mean transverse $B$ momentum is 5.3 GeV/c, virtually independent of the longitudinal momentum. Since they also suffer more multiple scattering, they have relatively poorer $L/\sigma_L$ distributions. LHC-b, on the other hand, does not benefit by going to higher momentum because, after a momentum of around 10 GeV/c (depending on the detector), $\sigma_L$ also increases linearly.

The efficacy of this geometry is illustrated by considering the distribution of the resolution on the $B$ decay length, $L$, for the decay $B^o \to \pi^+\pi^-$. Fig. 5 shows the r.m.s. errors in the decay length as a function of momentum; it also shows the momentum distribution of the $B$'s accepted by BTeV. The following features are noteworthy:

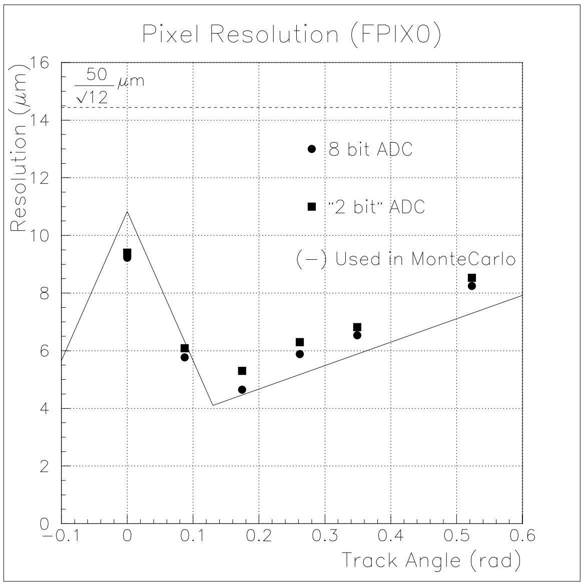


Figure 4: The resolution achieved in our test beam run using 50 $\mu$m wide pixels and an 8-bit ADC (circles) or a 2-bit ADC (squares), compared with our simulation (line).

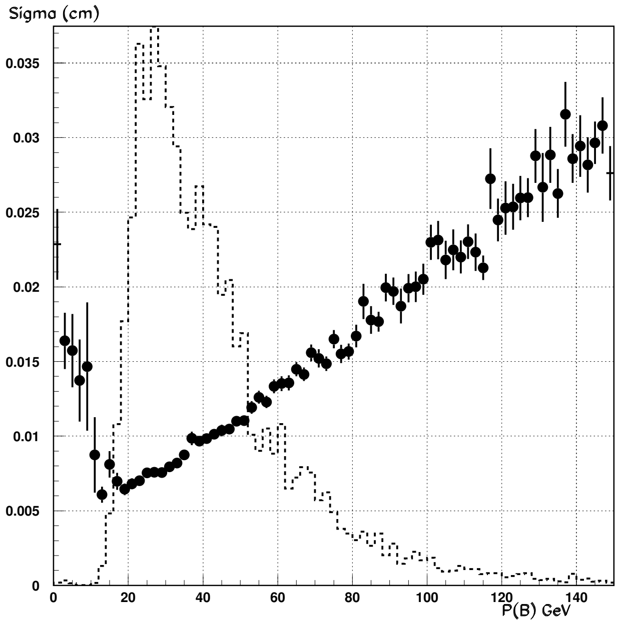


Figure 5: The $B$ momentum distribution for $B^o \to \pi^+\pi^-$ events (dashed) and the error in decay length $\sigma_L$ as a function of momentum.

Table 2: Level 1 trigger efficiencies for minimum-bias events and various processes of interest that are required to pass offline analysis cuts. All trigger efficiencies are determined for beam crossings with an average of two interactions per crossing using the Monte Carlo code shown in the table.

| Process | Eff. (%) | Monte Carlo |
|---|---|---|
| Minimum bias | 1 | BTeVGeant |
| $B_s \to D_s^+ K^-$ | 74 | BTeVGeant |
| $B^0 \to D^{*+} \rho^-$ | 64 | BTeVGeant |
| $B^0 \to \rho^0 \pi^0$ | 56 | BTeVGeant |
| $B^0 \to J/\psi K_s$ | 50 | BTeVGeant |
| $B_s \to J/\psi K^{*o}$ | 68 | MCFast |
| $B^- \to D^0 K^-$ | 70 | MCFast |
| $B^- \to K_s \pi^-$ | 27 | MCFast |
| $B^0 \to$ 2-body modes $(\pi^+\pi^-, K^+\pi^-, K^+K^-)$ | 63 | MCFast |

- The $B$'s used by BTeV peak at $p = 30$ GeV/c and average about 40 GeV/c.
- The decay length is equal to 450 $\mu$m $\times\, p/M_B$.
- The error on the decay length is smallest near the peak of our accepted momentum distribution. It increases at lower values of $p$, due to multiple scattering, and increases at larger values of $p$ due to the smaller angles of the Lorentz-boosted decay products.

## 4.3 The Detached Vertex Trigger

It is impossible to record data from each of the 7.5 million beam crossings per second. A prompt decision, colloquially called a "trigger," must be made to record or discard the data from each crossing. The main BTeV trigger is provided by the silicon pixel detector. The Level 1 Vertex Trigger inspects every beam crossing and, using only data from the pixel detector, reconstructs the primary vertices and determines whether there are detached tracks which could signify a $B$ decay. Since the $b$'s are at high momentum, the multiple scattering of the decay products is minimized allowing for triggering on detached heavy quark decay vertices.

With our outstanding pixel resolution, we are able to trigger efficiently at Level 1 on a variety of $b$ decays. The trigger has been fully simulated, including the pattern recognition code. In Table 2 we give the efficiencies to trigger on a sample of final states providing that the particles are in the detector acceptance and otherwise pass all the analysis cuts. We see the trigger efficiencies are generally above 50% for the $b$ decay states of interest and at the 1% level for minimum bias background. These numbers are evaluated at an average rate of 2 interactions per beam crossing, corresponding to our design luminosity of $2{\times}10^{32}$ cm$^{-2}$s$^{-1}$.

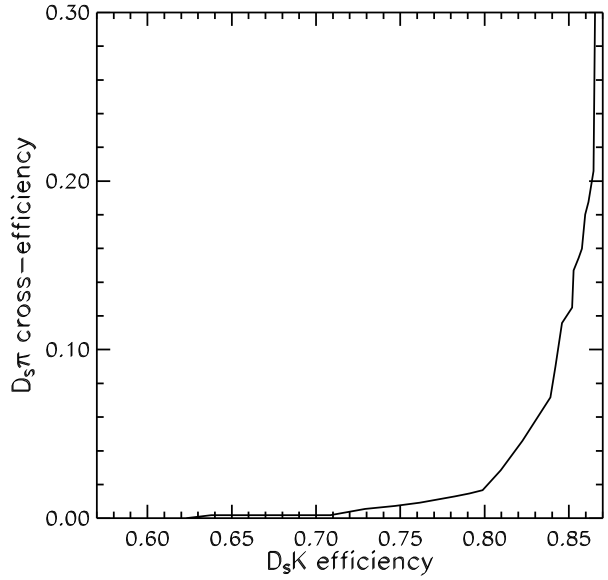


Figure 6: The efficiency to detect the fast $K^-$ in the reaction $B_s \to D_s^+ K^-$ versus the rate to misidentify the $\pi^-$ from $B_s \to D_s^+ \pi^-$ as a $K^-$.

## 4.4 Charged Particle Identification

Charged particle identification is an absolute requirement for a modern experiment designed to study the decays of $b$ and $c$ quarks. The relatively open forward geometry has sufficient space to install a Ring Imaging Cherenkov detector (RICH), which provides powerful particle ID capabilities over a broad range of momentum. The BTeV RICH detector must separate pions from kaons and protons in a momentum range from 3−70 GeV/$c$. The lower momentum limit is determined by soft kaons useful for flavor tagging, while the higher momentum limit is given by two-body $B$ decays. Separation is accomplished using a gaseous freon radiator to generate Cherenkov light in the optical frequency range. The light is then focused from mirrors onto Hybrid Photo-Diode (HPD) tubes. To separate kaons from protons below 10 GeV/c an aerogel radiator will be used.

As an example of the usefulness of this device we show, in Fig. 6, the efficiency for detecting the $K^-$ in the decay $B_s \to D_s^+ K^-$ versus the rejection for the $\pi^-$ in the decay $B_s \to D_s^+ \pi^-$. We see that high efficiencies can be obtained with excellent rejections.

## 4.5 Electromagnetic Calorimeter

In BTeV, photons and electrons are detected when they create an electromagnetic shower cascade in crystals of $PbWO_4$, a dense and transparent medium that produces scintillation light. The amount of light is proportional to the incident energy. The light is sensed by photomultiplier tubes (or possibly hybrid photodiodes). The crystals are 22 cm long and

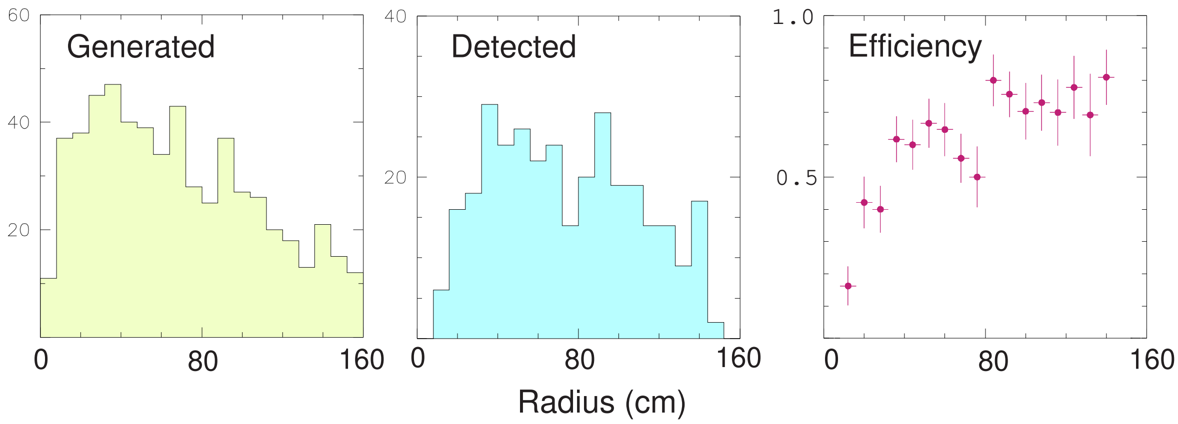


Figure 7: The radial distribution of generated and detected photons from $B^o \to K^*\gamma$ and the resulting efficiency. The detector was simulated by GEANT and the resulting crystal energies were clustered by our software. The charged tracks from the $K^*$ were required to hit the RICH. The simulation was run at 2 interactions/crossing.

have a small transverse cross-section, 26 mm$\times$ 26 mm, providing excellent segmentation. The energy and position resolutions are exquisite,

$$\frac{\sigma_E}{E} = \sqrt{\frac{(1.6\%)^2}{E} + (0.55\%)^2}\ , \quad (4)$$

$$\sigma_x = \sqrt{\frac{(3500\ \mu m)^2}{E} + (200\ \mu m)^2}\ , \quad (5)$$

where $E$ is in units of GeV. This leads to an r.m.s. $\pi^o$ mass resolution between 2 and 5 MeV/$c^2$ over the $\pi^o$ momentum range 1 to 40 GeV/c.

The crystals are designed to point at the center of the interaction region. They start at a radial distance of 10 cm with respect to the beam-line and extend out to 160 cm. They cover $\sim$210 mrad. This is smaller than the 300 mrad acceptance of the tracking detector; the choice was made to reduce costs. For most final states of interest this leads to a loss of approximately 20% in signal.

The calorimeter, at 2 interactions per crossing, has a high rate close to the beam pipe, where the reconstruction efficiency and resolution is degraded by overlaps with other tracks and photons. As we go out to larger radius, the acceptance becomes quite good. This can be seen by examining the efficiency of the $\gamma$ in the decay $B^o \to K^*\gamma$, $K^* \to K^-\pi^+$. Here the decay products of the $K^*$ are required to reach the RICH detector. Fig. 7 shows the radial distribution of the generated $\gamma$'s, the reconstructed $\gamma$'s and the $\gamma$ efficiency versus radius. The shower reconstruction code, described in Chapter 12 of the proposal, was developed from that used for the CLEO CsI calorimeter; for reference, the efficiency of the CLEO barrel electromagnetic calorimeter is 89%.

### 4.6 Forward Tracking System

The other components of the charged-particle tracking system are straw-tube wire proportional chambers and, near the beam where occupancies are high, silicon microstrip detectors. These devices are used primarily for track momentum measurement, $K_s$ detection and the Level 2 trigger. These detectors measure the deflection of charged particles by the BTeV analyzing magnet and give BTeV excellent mass and momentum resolution for charged particle decay modes.

### 4.7 Muon Detection

Muon detection is accomplished by insisting that the candidate charged track penetrate several interaction lengths of magnetized iron and insuring that the momentum determined from the bend in the toroid matches that given by the main spectrometer tracking system. The muon system is also used to trigger on the dimuon decays of the $J/\psi$. This is important not only to gather more signal but as a cross check on the efficiency of our main trigger, the Detached Vertex Trigger.

### 4.8 Data Acquisition System

BTeV has a data acquisition system (DAQ) which is capable of recording a very large number of events. The full rate of $B$'s whose decay products are in the detector is very high, over 1 kHz. The (direct) charm rate is similar. Other experiments are forced by the limitations of their data acquisition system to make very harsh decisions on which $B$ events to take. BTeV can record nearly all the potentially interesting $B$ and charm candidates in its acceptance. Therefore it can address many topics that might be discarded by an experiment whose DAQ is more restrictive. Since nature has a way of surprising us, we view the open nature of the BTeV trigger and the capability of the DAQ as a genuine strength that offers us the opportunity to learn something new and unanticipated.

## 5 Simulation Results and Physics Reach

The physics reach of BTeV has been established by an extensive and sophisticated program of simulations, which is described in detail in Part 3 of the proposal. We have simulated the efficiencies and backgrounds in the decay modes used to measure the CP violating angles $\alpha$, $\beta$, $\gamma$ and $\chi$, the $B_s$ mixing parameter $x_s$ and a few rare decay final states.

We have used two simulation packages, GEANT and MCFast. These tools and their use are explained in the beginning of Part III. Briefly, GEANT models all physical interactions of particles with material and allows us to see the effects of hard to calculate backgrounds. The goal of MCFast is to provide a fast, parametrized simulation which is more flexible than GEANT but not quite as complete in its modeling of physics processes.

Table 3: Summary of physics reach in $10^7$s. Pairs of reactions between two lines are used together.

| Process | # of Events | $S/B$ | Parameter | Error or (Value) |
|---|---|---|---|---|
| $B^o \to \pi^+\pi^-$ | 24,000 | 3 | Asym. | 0.024 |
| $B_s \to D_s^{\pm} K^{\mp}$ | 13,100 | 7 | $\gamma$ | $7^\circ$ |
| $B^o \to J/\psi K_S$ | 80,500 | 10 | $\sin(2\beta)$ | 0.025 |
| $B_s \to D_s^+\pi^-$ | 103,000 | 3 | $x_s$ | (75) |
| $B^- \to \overline{D}^0(K^+\pi^-)K^-$ | 300 | 1 | $\gamma$ | $10^\circ$ |
| $B^- \to D^0(K^+K^-)K^-$ | 1,800 | >10 | $\gamma$ | $10^\circ$ |
| $B^- \to K_S\pi^-$ | 8,000 | 1 | $\gamma$ | $< 5^\circ$ |
| $B^o \to K^+\pi^-$ | 108,000 | 20 | $\gamma$ | $< 5^\circ$ |
| $B^o \to \rho^{\pm}\pi^{\mp}$ | 9,400 | 4.1 | $\alpha$ | $\sim 10^\circ$ |
| $B^o \to \rho^o\pi^o$ | 1,350 | 0.3 | $\alpha$ | $\sim 10^\circ$ |
| $B_s \to J/\psi\eta$ | 1,920 | 15 | $\sin(2\chi)$ | 0.033 |
| $B_s \to J/\psi\eta'$ | 7,280 | 30 | $\sin(2\chi)$ | 0.033 |
| $B^- \to K^-\mu^+\mu^-$ | 1280 | 3.2 | | |
| $B^o \to K^*\mu^+\mu^-$ | 2200 | 10 | | |

In Table 3 we give the decay mode, the number of signal events found in $10^7$ seconds at a luminosity of $2 \times 10^{32}$ cm$^{-2}$s$^{-1}$ and the signal/background ratio for many of the interesting decay modes which are possible for BTeV. We also estimate the error in the relevant physics parameter, if possible, or the reach in $B_s$ mixing. In some cases more than one reaction is used to determine a value; in that case they are put between horizontal lines.

Fig. 8 shows the power of an $L/\sigma_L$ cut on reducing prompt backgrounds in order to extract a clean $B \to J/\psi K_s^o$ signal. This rejection power comes from the forward geometry combined with excellent vertex resolution. Fig. 9 shows the superb capabilities of the electromagnetic calorimeter in detecting photons that are used to reconstruct $\eta$ and $\eta'$ candidates, which can be combined with $J/\psi$'s to measure $\chi$ through the state $B_s \to J/\psi\eta^{(')}$. Fig. 10 shows the decay mode $B_s \to D_s K$ signal which can be used to measure $\gamma$. The $\pi^+\pi^-\pi^o$ invariant mass distributions for $B \to \rho\pi$ signal and background are shown in Fig. 11. The $B \to \rho\pi$ decay can be used to measure $\alpha$.

The physics reach of BTeV is extraordinary, even in just one year of running. BTeV will be the first to make a precision measurement of the angle $\gamma$; this will be accomplished in one year of running. The angles $\alpha$ and $\chi$ will also be measured, though this will take a bit longer. The $B_s$ mixing reach is up to $x_s$ of 75, well above the Standard Model allowed range of about 40. Thus, not only can BTeV measure the value in the Standard Model, but it also has a good chance to measure $B_s$ mixing if it is determined by physics beyond the Standard Model. Non-Standard Model physics can also be seen via rare decays where large numbers of reconstructed events are expected.

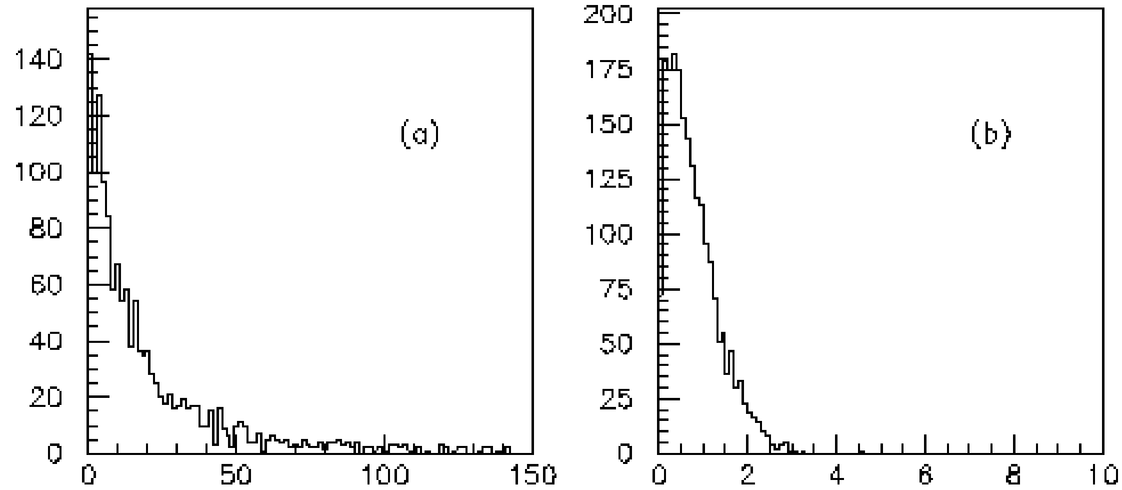


Figure 8: Distributions of $L/\sigma_L$ for (a) $J/\psi$ candidates from $B^o \to J/\psi K_s$ and (b) prompt $J/\psi$ candidates. The prompt candidates are suppressed by requiring $L/\sigma_L > 4$.

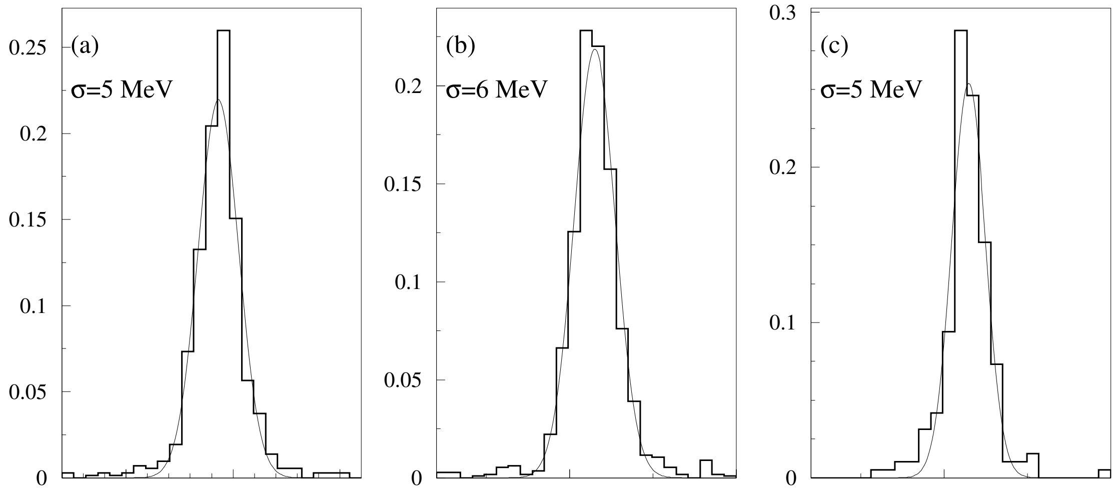


Figure 9: The invariant mass distributions for (a) $\eta \to \gamma\gamma$, (b) $\eta' \to \pi^+\pi^-\gamma$, and $\eta' \to \pi^+\pi^-\eta$, $\eta \to \gamma\gamma$. The Gaussian mass resolutions are indicated. $\eta$ and $\eta'$ candidates can be used to measure $\chi$ using the decay mode $B_s \to J/\psi\eta'$ and $B_s \to J/\psi\eta$.

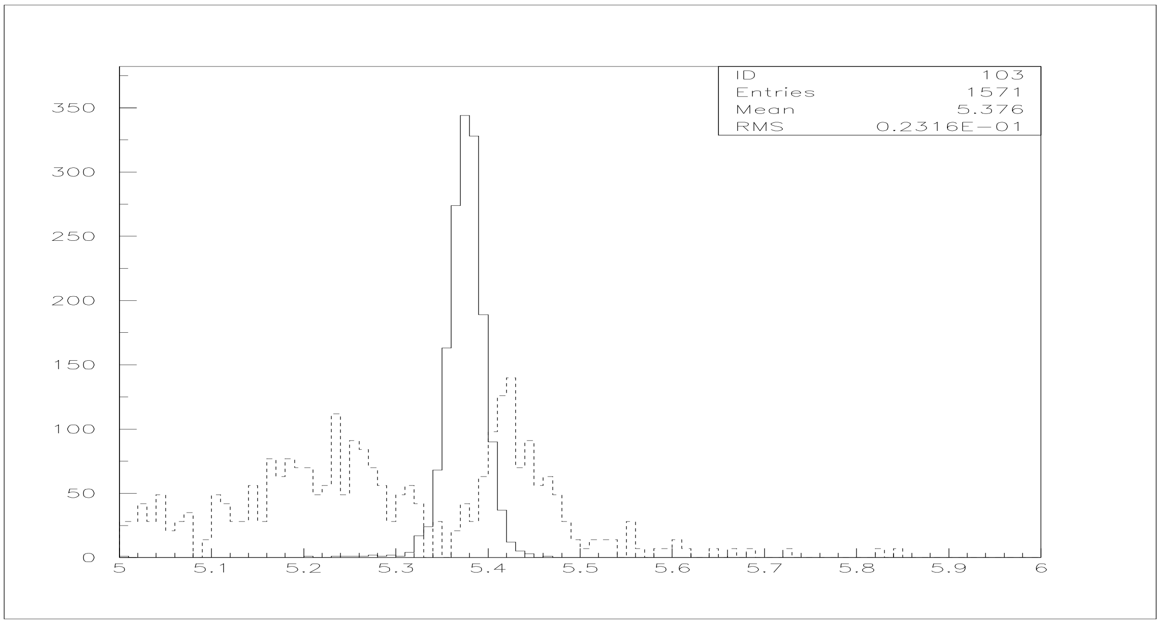


Figure 10: Comparison of $B_s \to D_s^+ K^-$ signal and background from $B_s \to D_s X$, where X contains at least one pion misidentified as a $K^-$. This state is used to measure $\gamma$.

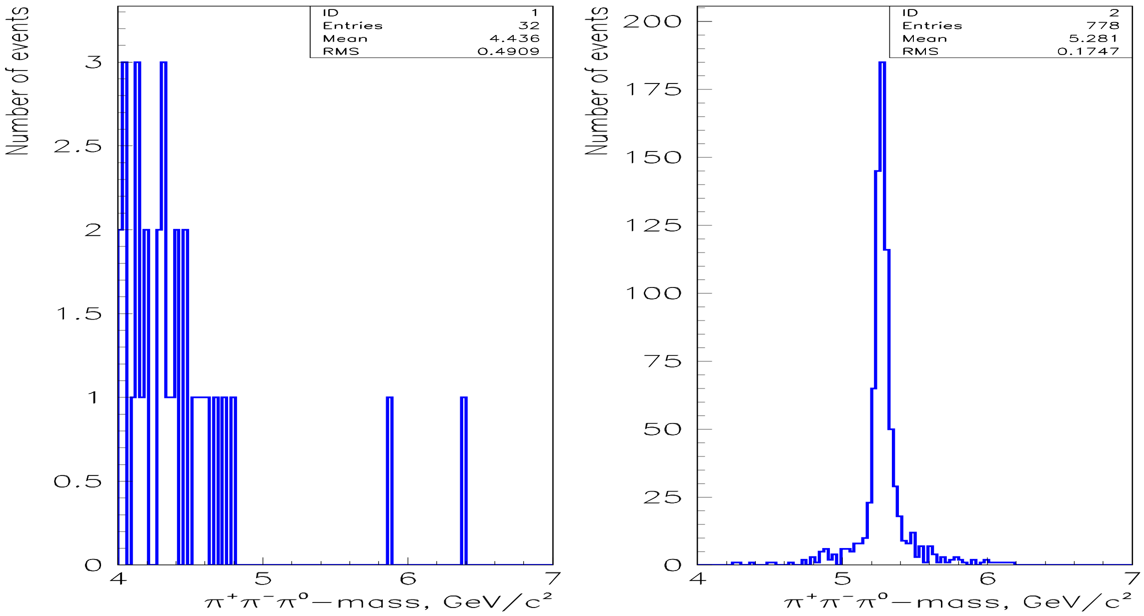


Figure 11: Invariant $\pi^+\pi^-\pi^o$ mass distributions for background (left) and signal (right) events for $B \to \rho^+\pi^-$. This state is used to measure $\alpha$. (The background is not normalized to the signal).

# 6 Comparisons With Other Experiments

BTeV compares favorably to all other heavy quark experiments.

BTeV has considerably more reach in every physics channel than $e^+e^-$ $B$ factories. We give one example here. Table 4 shows a comparison between BTeV and an asymmetric $e^+e^-$ machine for measuring the CP violating asymmetry in the decay mode $B^o \to \pi^+\pi^-$. It is clear that the large hadronic $b$ production cross section can overwhelm the much smaller $e^+e^-$ rate. Furthermore, the $e^+e^-$ $B$ factories do not have access to the important CP violation measurements that need to be made in $B_s$ decays. Nor can they explore potentially interesting topics in the physics of $b$-baryons and $B_c$ mesons.

Table 4: Number of tagged $B^o \to \pi^+\pi^-$ ($\mathcal{B}$=0.43 $\times 10^{-5}$).

| | $\mathcal{L}$(cm$^{-2}$s$^{-1}$) | $\sigma$ | # $B^o/10^7$ s | Signal Efficiency | Tagging $\epsilon D^2$ | # Tagged/$10^7$ s |
|---|---|---|---|---|---|---|
| $e^+e^-$ | $3 \times 10^{33}$ | 1.2 nb | $3.6 \times 10^7$ | 0.3 | 0.3 | 13 |
| BTeV | $2 \times 10^{32}$ | 100$\mu$b | $1.5 \times 10^{11}$ | 0.037 | 0.1 | 2370 |

CDF and D0 have done useful $b$ physics by triggering on $J/\psi$ decays into dimuons. CDF plans more aggressive triggers on selected purely hadronic final states in the future. However, the kinematics of $b$ decays do not favor the central region. Most of the $b$'s are relatively slow with the peak of the transverse momentum distribution being at 5.3 GeV/c, which at an $\eta$ of 1, produces $B$'s with $\gamma\beta$ of 1. These relatively slow $B$'s are intrinsically difficult to vertex and trigger on. Furthermore, CDF and D0 do not have state of the art charged particle identification nor do they possess excellent photon detection.

Although the ATLAS and CMS detectors will have some $b$ physics capabilities, they will be limited to final states with dileptons or even perhaps only to $J/\psi$ decays. LHC-b, on the other hand, is an experiment that has been designed exclusively to study $b$ decays and provides real competition in many areas. Our simulations show that we expect larger yields than LHC-b in all charged particle final states, at comparable or better signal-to-noise ratios, and we have large advantages in final states with photons.

For example, we compare the reaction $B^o \to \rho\pi$ in Table 5. Both sets of numbers are calculated for $10^7$ seconds at a luminosity of $2 \times 10^{32}$ cm$^{-2}$s$^{-1}$. We have corrected the LHC-b numbers by normalizing them to the branching ratios used by BTeV.

Furthermore, we intend to output on the order of 5 times more $b$'s per second than LHC-b allowing for a greater range of physics studies. We also have the capacity in our data acquisition system to accept a large number of directly produced charm decays.

Table 5: Event yields and signal/background for $B^o \to \rho\pi$.

| Mode | Branching Ratio | BTeV | | LHC-b | |
|---|---|---|---|---|---|
| | | Yield | S/B | Yield | S/B |
| $B^o \to \rho^{\pm}\pi^{\mp}$ | $2.8\times10^{-5}$ | 9400 | 4.1 | 2140 | 0.8 |
| $B^o \to \rho^o\pi^0$ | $0.5\times10^{-5}$ | 1350 | 0.3 | 880 | - |

# 7 Costs and Schedule

The BTeV proposal is accompanied by a detailed Work Breakdown Structure (WBS) and cost estimate.

## 7.1 Costs

Since BTeV is only at the proposal submission stage, we do not have complete engineering designs for our systems. However, we have a complete and stable baseline design and an active program of R&D on all parts of the detector. Many of our systems are similar to ones that have been built recently or are being built for future experiments. We have drawn on our own experience, and that of others, with these types of systems to develop the cost estimate for BTeV. In many cases, the large cost drivers are procurements and, for these, we have had direct discussions with vendors and have obtained price quotes. Where chip development is required, we have consulted with engineers concerning the number of prototype cycles required. Our cost estimate includes all labor costs and tries to account for inflation, industry trends and contingency. We also include the costs of our R&D program as well as project management and ES&H costs. The high level rollup of the costs for detector construction and offline computing are given in Tables 6 and 7.

## 7.2 Schedule

The BTeV program is an ambitious one. Its goal is to begin data taking in 2005/6. This timing is well-matched to the world $B$ physics program. The $e^+e^-$ $B$ factories and the Fermilab collider experiments will have had several years of running, the first results in, and their significance thoroughly digested. It should be clear what the next set of goals is and BTeV will be guaranteed to be well-positioned to attack them. This schedule also gives BTeV a good opportunity to have a head start in its inevitable competition with LHC-b, especially since BTeV can be installing and operating components of its detector in the collision hall well in advance of 2005. Finally, this schedule is sensibly related to our plan to conduct a rigorous R&D program which includes a sequence of engineering runs to test the technically challenging systems in our design. We believe that the scale of the BTeV construction effort is comparable to the scale of one of the current detector upgrades. The time scale is comparable as well.

Table 6: Baseline BTeV detector cost estimate ($).

| Item | Cost ($) BTeV Baseline |
|---|---|
| Magnets, beampipes | 1.80 M |
| Pixels | 14.25 M |
| RICH | 17.14 M |
| EM Calorimeter | 21.02 M |
| Muon | 6.72 M |
| Straw Tubes | 12.14 M |
| Silicon Strips | 5.10 M |
| Trigger Level 1 | 6.20 M |
| DAQ+links | 4.82 M |
| Level 2/3 | 2.95 M |
| Controls/timing | 1.97 M |
| Control room | 1.16 M |
| DAQ software | 2.87 M |
| Test stands | 1.62 M |
| Installation, commissioning | 1.45 M |
| Project management | 3.86 M |
| Total | 105.07 M |

Table 7: Preliminary BTeV offline computing cost estimate ($).

| Item | Cost ($) Baseline |
|---|---|
| Hardware | 5.3 M |
| Software Dev. | 7.1 M |
| Total | 12.4 M |

# 8 Conclusion

BTeV is a powerful and precise scientific instrument capable of exquisite tests of the Standard Model. It has great potential to discover new physics via rare or CP violating decays of heavy quarks.

# References

[1] N. Cabibbo, *Phys. Rev. Lett.* **10**, 531 (1963); M. Kobayashi and K. Maskawa, *Prog. Theor. Phys.* **49**, 652 (1973).

[2] R. Aleksan, B. Kayser and D. London, Phys. Rev. Lett. 73 (1994) 18 (hep-ph/9403341).

[3] F. Abe *et al.*, "Measurement of the $B$ Meson Differential Cross-Section in $p\overline{p}$ collisions at $\sqrt{s}$ = 1.8 TeV," CDF/PUB/BOTTOM/PUBLIC/3759 submitted to ICHEP '96 and references therein; F. Abe *et al.*, *Phys. Rev. Lett.* **75**, 1451 (1995); R. Abbott *et al.*, "The $b\overline{b}$ Production Cross Section and Angular Correlations in $p\overline{p}$ collisions at $\sqrt{s}$ = 1.8 TeV," FERMILAB-Pub-99/144-E; S. Abachi *et al*, *Phys. Rev. Lett.* **74**, 3548 (1995).

[4] D. Fein, "Tevatron Results on $b$-Quark Cross Sections and Correlations," presented at Hadron Collider Physics (HCP99) (Bombay), January 1999.